NEAL-SMITH CRITERIA-BASED H_∞-APPROACH TO PREDICTING AIRCRAFT HANDLING QUALITIES

Norihiro Goto*
Kyushu University, Fukuoka 812-8581, Japan
E-mail : goto@aero.kyushu-u.ac.jp
Takayuki Hoshizaki†
Purdue University, West Lafayette, Indiana 47907-1282, U.S.A.

Keywords: *Neal-Smith criteria, H_∞-model, control rate*

Abstract

The Neal-Smith criteria for assessing handling qualities of highly augmented aircraft have been transformed into an H_∞-mixed-sensitivity norm. The norm features a control rate related term to account for the roll-off characteristic of the human pilot. The pitch attitude control is formulated as a mixed-sensitivity problem, which is solved by the model matching technique to yield H_∞-optimal pilot models. It is shown that the H_∞-optimal pilot models well characterize the human pilot's linear control behavior, and the resulting complementary sensitivity function meets the Neal-Smith criteria satisfactorily. Based on this result, a method is proposed to correlate the pilot rating data of the Neal-Smith flight test with the pilot compensation efforts manifested by the H_∞-optimal pilot model. It is shown that a pair of measures from the H_∞-optimal pilot model, maximum gain gradient and phase at the bandwidth frequency, can clearly divide the experimental pilot ratings into three levels.

1. Introduction

There exist several methods for evaluating the short-term small-amplitude pitch response demonstrated by highly augmented aircraft[1]. Above all, the Neal-Smith method[2]is the benchmark with which other methods are compared. The method is based on the Neal-Smith criteria stating that pilot rating is primarily a function of the pilot's compensation required to achieve good low-frequency performance and the closed-loop oscillatory tendencies that result. In the method, the pilot compensation that meets the criteria is found either graphically[2] or analytically by solving an optimization problem[3] with the use of an assumed simple pilot model. Thus, the method has incurred difficulties in uniquely determining the pilot compensation efforts exerted by a realistic pilot in charge of control. Employing the optimal control approach to modeling the pilot loop closures is one way to cope with the difficulties. In this approach, the Neal-Smith criteria are reflected in the resulting optimal control model (OCM) of the pilot[4], while the performance index itself is not a manifestation of the criteria.

In an attempt at forming a performance index out of the Neal-Smith criteria, and thereby finding a unique pilot model and pilot compensation, Ref.5 proposes the H_∞-modeling technique, in which the Neal-Smith criteria are transformed into a mixed-sensitivity norm in the framework of the H_∞-control theory. Minimization of the norm yields the H_∞-optimal pilot model, which in turn is used to define the pilot compensation efforts for the task. It is shown in Refs.5 and 6 that a pair of measures manifested by the H_∞-optimal pilot model, maximum gain gradient within the frequency range of interest and the phase compensation at the bandwidth frequency, correlates well with experimental pilot ratings in terms of level division for pitch attitude

*Professor, Department of Aeronautics and Astronautics.
Associate Fellow AIAA.
†Graduate Student, School of Aeronautics and Astronautics.

tracking single-loop tasks such as those in the Neal-Smith flight test. It is pointed out in Ref.5, however, that the H_∞-optimal pilot model developed there is not strictly indicative of the human pilot behavior, particularly in that it does not show the first-order roll-off characteristic in a high-frequency range that is inherent in human pilots. The H_∞-modeling approach needs to be improved and tested against measured pilot control behavior.

Therefore, the primary objective of this paper is to refine the H_∞-norm so that its minimization yields H_∞-optimal pilot models that are more indicative of the human pilot behavior. Then, the correlation of the H_∞-optimal pilot compensation with experimental pilot ratings is discussed in terms of the aforementioned two measures in comparison with the result of Ref.5.

2. Improved H_∞-Norm

The pitch attitude tracking feedback system under consideration is shown in Fig.1, where $Y_p(s)$ denotes the pilot transfer function, $H(s)$ does the aircraft transfer function from an elevator stick force F_s to the pitch attitude θ response including a flight control system (FCS), and s is the Laplace transform parameter. Define the closed-loop transfer functions as

$S = \theta_e/\theta_c$: sensitivity function (1)

and

$T = \theta/\theta_c$: complementary sensitivity function. (2)

Using T, the Neal-Smith criteria can be itemized as follows:

(a) Define the task-dependent bandwidth frequency ω_b, where

$$\angle T = -90 \ \text{deg}. \tag{3}$$

(b) Minimize the low-frequency droop of T, or desirably

$$|T| \geq \text{-3dB} \ \text{ for } \ \omega \leq \omega_b. \tag{4}$$

(b) Minimize the resonant peak in the high-frequency range, or

$$\text{minimize } |T|_{\max} \ \text{ for } \ \omega \geq \omega_b. \tag{5}$$

The low-frequency requirement (b) is concerned with the tracking performance. If the performance is interpreted as the mean square value of θ_e to the mean square value of a random input θ_c, the performance is bounded by $\sup_\omega |S(j\omega)|^2$. Therefore, the criterion (b) is replaced here by

$$\text{minimize } |S|_{\max} \ \text{ for } \ \omega \leq \omega_b. \tag{6}$$

Because the criterion (6) does not guarantee the minimization of the droop, shaping of $|T|$ is taken into consideration through the related weighting function to be described later.

In addition to the requirements of (5) and (6), an improvement to be made here is the inclusion in the performance index of a control rate related term which the standard OCM approach contains in order to account for the human pilot's neuromuscular lag. This type of control rate term is also included in the H_∞-norm of Ref.7 succeeding in obtaining a good match with experimental describing functions as well as conventional OCMs. Note that this paper's approach differs from that of Ref.7 in that frequency-shaped weighting functions are used in order to well represent the Neal-Smith criteria.

Putting together the requirements (5) and (6) and the control rate related term, an improved H_∞-performance index can be defined here as

$$\lambda^2 = \inf_{\text{stabilizing } Y_p(j\omega)} \left\| |V(j\omega)S(j\omega)|^2 + |W(j\omega)T(j\omega)|^2 + |\mu(j\omega)\dot{Q}(j\omega)|^2 \right\|_\infty \tag{7}$$

where

$$j = \sqrt{-1},$$

$$\left\| \bullet(j\omega) \right\|_\infty = \sup_\omega \left| \bullet(j\omega) \right|, \tag{8}$$

$\dot{Q}(s) = s F_s/\theta_c$: closed-loop control rate transfer function, (9)

and λ is the optimal value of the performance index which should be smaller than 1. $V(j\omega)$, $W(j\omega)$ and $\mu(j\omega)$ are suitably chosen weighting functions having the roles of shaping

S, T and $\dot{Q}$, respectively. The problem of finding the optimal controller in the sense of Eq.(7) can be reduced to a model matching problem[8] as described in Appendix.

3. Weighting Functions

Because the weighting functions $V(j\omega)$ and $W(j\omega)$ have to express the implications of the Neal-Smith criteria, they must be chosen carefully. In explicit terms, they are required to shape S and T in such a way that

$$|S(j\omega)| \le |V^{-1}(j\omega)| \le D \text{ for } \omega \le \omega_b \quad (10)$$

$$|T(j\omega)| \le |W^{-1}(j\omega)| \text{ for } \omega \ge \omega_b . \quad (11)$$

In inequality (10), the upper bound D is set here as a constant such that the resulting pilot model has a reasonable low-frequency gain level. Minimizing the droop is taken care of by shaping T through the weighting function W. The weighting function $\mu(s)$ should be designed so that $s\mu(s)$ be proper as shown in Appendix.

The choice of the weighting functions compatible with these conditions is not unique. Referring to Ref.5, and as a result of testing several combinations of the weighting functions[5, 9], the following forms are selected here:

$$V(s) = \frac{\tau_{V_2} s + 1}{\tau_{V1} s} \quad (12)$$

$$W(s) = \kappa_W (\tau_W s + 1) \quad (13)$$

$$\mu(s) = \frac{g}{1 + \tau_\mu s} \quad (14)$$

where

$$\tau_{V_2} = \tau_W = 1/\omega_b \quad (15)$$

from the condition that ω_b be the boundary frequency that distinguishes between a low-frequency range and a high-frequency range. The employment of the first-order form of $W(s)$ in Eq.(13) instead of the second-order form in Ref.5 is due to the realization of the –20dB/dec roll-off characteristic of the human pilot in a high-frequency range. The value of D dB in inequality (10) together with that of κ_W is adjusted so that the resulting H_∞-optimal pilot models have about 5dB low-frequency gain levels. Note, however, that this way of gain adjustment is not essential in correlating pilot compensation efforts with pilot ratings. Actual values of D and κ_W used in the analysis are

$$D \cong 2.1 \text{ dB} \quad (16)$$

$$\kappa_W = 10^{-30/20}. \quad (17)$$

Following Ref.5, the value of τ_{V1} is determined by

$$\tau_{V_1} = 10^{D/20} \sqrt{2}/\omega_b . \quad (18)$$

Note that the condition (10) is stricter in this work than in Ref.5 where D=3dB is set. The constant g in Eq.(14) is determined iteratively in the analysis so that the condition that $\angle T = -90$ deg at $\omega = \omega_b$ can be attained, while the time constant τ_μ is allotted a very small value of 10^{-5}, because the role of $\mu(s)$ is merely to make $s\mu(s)$ proper. The bandwidth frequency ω_b is treated in this work as a variable, which is adjusted in such a way that the roll-off starts at around 10.0 rad/s. Although in the original work by Neal and Smith[2] the bandwidth frequency is given a fixed-value that depends on the indicated airspeed, it is in actuality a variable internally set by the pilot in each task so that he or she can keep a high-gain control to attain a good low-frequency performance. Summarizing, determination of the weighting function-related parameters is made along the iterative procedure to follow:

Step1 : Start computation with an arbitrary set of (ω_b, g), and change g up until $\angle T|_{\omega_b} \cong -90$ deg.

Step2 : Change ω_b so that the roll-off starts at around 10 rad/s.

Step3 : Readjust g so that $\angle T|_{\omega_b} = -90$ deg.

Step4 : Go back to Step2 to check the roll-off condition.

It turns out that a few cycles of the iteration are enough for the parameter values to converge to those shown in Table 1 which also summarizes the Neal-Smith test parameters.

Two remarks are in order for the actual analysis of the H_∞-optimal problem. First, the

condition on the model matching technique that the plant $H(s)$ be free of poles or zeros on the imaginary axis is approximately satisfied by perturbing them slightly to the left-half plane of s : the pole s=0 of $H(s)$ in Fig.1 is replaced by $s=-\varepsilon$ (ε>0,small). Second, the time delay term, $e^{-\tau s}$, inherent in the pilot transfer function $Y_p(s)$, is first regarded as part of the plant $H(s)$. After finding an H_∞-optimal controller $G(s)$ exclusive of the delay term, it is recombined with the delay term to make up $Y_p(s)$, as implied by the following open-loop transfer function :

$$L(s)=Y_p(s)H(s)=(G(s)e^{-\tau s})H(s)$$
$$=G(s)\tilde{H}(s) \qquad (19)$$

where

$$\tilde{H}(s)=H(s)e^{-\tau s}.$$

In the analysis, the transcendental term is replaced by the Pade approximation, and the delay time τ is fixed at the same value as is used in Ref.2 ; that is,

$$e^{-\tau s}=(1-\frac{\tau s}{2})\Big/(1+\frac{\tau s}{2}) \qquad (20)$$

$$\tau=0.3\ s. \qquad (21)$$

Rigorous handling of the delay term is possible[9]. It turns out, however, that the effect of the Pade approximation is very small in the frequency range of interest.

4. H_∞-Pilot Models

The aircraft transfer function treated here is given by

$$H(s)=H_\Theta(s)H_F(s) \qquad (22)$$

where the constant-speed transfer function of the pitch attitude to stick force is

$$H_\Theta(s)=\frac{K_\theta(\tau_{\theta_2}s+1)}{s(s^2/\omega_{sp}^{\ 2}+2\zeta_{sp}\,s/\omega_{sp}+1)} \qquad (23)$$

and the FCS transfer function is

$$H_F(s)=\frac{\tau_1 s+1}{(\tau_2 s+1)(s^2/\omega_\varepsilon^{\ 2}+2\zeta_\varepsilon\,s/\omega_\varepsilon+1)} \qquad (24)$$

Sets of the parameters in Eqs.(23) and (24) and the flight configuration number assigned to each set are summarized in Table 1 together with the pilot rating data of the Neal-Smith flight test and the H_∞-optimal values of ω_b, g and λ that have resulted from this work.

Using the weighting functions of Eqs.(12), (13) and (14) and the computational procedure described in the previous section, H_∞-optimal pilot models have been computed for all of the flight configurations of Table 1. In Fig.2 are shown representative H_∞-optimal S and T ; Fig.2a is for the configuration 2D which is rated almost the best in Table 1, and Fig.2b is for 5C which is given one of the worst ratings. Although these H_∞-optimal S and T depend on the configuration because the bandwidth frequency ω_b and the constant g are variables here unlike Ref.5 which employs fixed ω_b's and lacks the g-related term in the H_∞-norm, Fig.2 shows that the Neal-Smith criteria are well satisfied. A resonant peak can be noticed in T of Fig.2b. Noting, however, that the peak value is below 0dB, it can rather be said that a high-frequency droop has come about. This feature can be found for the configurations of poor pilot ratings such as 2I and 5A~5E.

Figure 3 shows typical examples of the H_∞-optimal pilot models : those for the flight configurations 1F, 2D, 3A, and 5C of Table 1. Except for the roll-off characteristic beyond 10 rad/s, they exhibit similar features to those shown in Ref.5. These results can be itemized as follows :

1. Neal-Smith criteria can be well satisfied by the weighting functions, Eqs.(12), (13) and (14).
2. High-frequency roll-off characteristic of the human pilot can be well represented by the control rate term in the performance index.
3. Inclusion of the control rate term in the performance index makes little difference in the low-frequency features of the H_∞-optimal pilot models.
4. However, inclusion of the roll-off characteristic brings a lowering of the bandwidth frequency.

5. Correlation with Pilot Ratings

Drawing on the above-mentioned results, it is attempted here to divide the pilot rating data of

Table 1 into three levels with the use of the same two measures concerning the pilot compensation efforts as are introduced in Ref.5 ; i.e. , the phase compensation of the H_∞-optimal pilot model at the bandwidth frequency including the time delay term

$$\angle Y_P(j\omega)|_{\omega b} \text{ deg} \tag{25}$$

and the maximum gain gradient of the H_∞-optimal pilot model within the frequency range of interest

$$\max\left[\Delta|Y_p|/\Delta\log\omega\right] \text{ dB/dec.} \tag{26}$$

Inclusion of the time delay term for evaluating Eq.(25) is due to the reason that ω_b differs from task to task, and therefore the phase lag due to the delay term depends on the specific ω_b. The frequency range of interest for getting Eq.(26) is specified as below 10 rad/s for the series 1~7 and below 16.5 rad/s ($=\omega_{sp}$) for the series 8 of Table 1. Figure 4 shows the result of the level division. In Fig.4, each pilot rating is the arithmetic mean of all of the ratings given to the particular configuration. Note that the boundary between levels 1 and 2 is the same as that in Ref.5, while the level 2 region is expanded toward a greater maximum gradient. In essence, taking into account the roll-off characteristic of the human pilot has little effect on the pilot's low-frequency compensation efforts, and therefore the two measures of Eqs.(25) and (26) work satisfactorily to divide the pilot rating data into three levels.

6. Conclusion

The H_∞-norm based on the Neal-Smith criteria has been improved so that it includes a control rate related term to account for the roll-off characteristic in a high-frequency range of the human pilot. The H_∞-optimal problem is solved by the model matching technique with the bandwidth frequency and the weight on the control rate term in the H_∞-norm as variables to yield H_∞-optimal pilot models for the Neal-Smith flight test configurations. The H_∞-optimal complementary sensitivity function meets the Neal-Smith criteria so well that the task difficulty is exhibited solely by the H_∞-optimal pilot models. It is demonstrated that the use of two measures from the H_∞-optimal pilot model, phase compensation at the bandwidth frequency and maximum gain gradient within the frequency range of interest, is successful in dividing experimental pilot ratings into three levels. This H_∞-modeling technique is to be applied to other flight test results than the Neal-Smith's.

References

[1] Hoh, R.H., and Mitchell, D.G., "Handling-qualities specification-a functional requirement for the flight control system," *Advances in Aircraft Flight Control*, Ed. Tischler, M. B., Taylor and Francis, London, pp.3-33, 1996.

[2] Neal, T.P., and Smith, R.E., "An In-Flight Investigation to Develop Control System Design Criteria for Fighter Airplanes," Air Force Flight Dynamics Lab., AFFDL-TR-70-74, Vols.1 and 2, Wright-Patterson AFB, OH, Dec. 1970.

[3] Kish, B.A., and Jones, B.L., " A Comparison of the Neal-Smith and $\omega_{sp}T_{\theta 2}, \zeta_{sp}, \tau_\theta$ Flying Qualities Criteria," AIAA Paper 95-3455, 1995.

[4] Bacon, B.J., and Schmidt, D.K., "An Optimal Control Approach to Pilot/Vehicle Analysis and the Neal-Smith Criteria," *Journal of Guidance, Control, and Dynamics*, Vol.6, No.5, pp.339-347, 1983.

[5] Goto, N., "Neal-Smith Criteria-Based H_∞-Modeling Technique for Assessing Pilot Rating," *Journal of Guidance, Control, and Dynamics*, Vol.21, No.4, pp.656-661, 1998.

[6] Goto, N., and Hoshizaki, T., "Extension of the Neal-Smith Criteria-Based H_∞-Modeling Technique to LAHOS Data, "*Proc. of AIAA Atmospheric Flight Mechanics Conference*, CP9808, pp.163-173, 1998.

[7] Anderson, M.R., "Standard Optimal Pilot Models," *Proc. of AIAA Guidance, Navigation, and Control Conference*, pp.750-756, 1994.

[8] Doyle, J.C., Francis, B.A., and Tannenbaum, A.R., *Feedback Control Theory*, Macmillan, New York, Chap.9, 1992.

[9] Goto,N., Chatani, K., and Fujita, S., " H_∞-Model of the Human Pilot Controlling Unstable Aircraft," *Proc. of the 1995 IEEE International Conference on Systems, Man, and Cybernetics* (Vancouver, BC, Canada), pp.2657-2662, 1995.

[10] Francis, B.A., *A Course in H_∞ Control Theory*, Springer-Verlag, Berlin, Chaps.6, 8, 1987.

[11] Kleinman, D.L., Baron, S., and Levison, W.H., "An Optimal Control Model of Human Response, Pt.I&II," *Automatica*, Vol.6, pp.357-383,1970.

Table 1 Neal-Smith flight test configuration summary and H_∞-pilot model parameters

Configuration	$1/\tau_1$	$1/\tau_{\theta 2}$	$1/\tau_2$	ω_{sp}/ζ_{sp}	$\omega_\varepsilon/\zeta_\varepsilon$	Pilot rating	H_∞-model parameters ω_b	g	λ
1A	0.5	1.25	2.0	2.2/0.69	63.0/0.75	2~6	2.18	0.042	0.995
1B	2.0	1.25	5.0	2.2/0.69	63.0/0.75	3~3.5	2.20	0.023	0.995
1C	2.0	1.25	5.0	2.2/0.69	16.0/0.75	2~5	2.20	0.013	0.9998
1D	∞	1.25	∞	2.2/0.69	75.0/0.67	3~5	2.30	0.008	0.995
1E	∞	1.25	5.0	2.2/0.69	63.0/0.75	6	2.30	0.002	0.996
1F	∞	1.25	2.0	2.2/0.69	63.0/0.75	8	2.25	0.001	0.996
1G	∞	1.25	0.5	2.2/0.69	63.0/0.75	8.5	2.20	0.0003	0.996
2A	2.0	1.25	5.0	4.9/0.7	63.0/0.75	4~4.5	2.20	0.1	0.997
2B	2.0	1.25	5.0	4.9/0.7	16.0/0.75	2.5~6	2.20	0.057	0.996
2C	5.0	1.25	12.0	4.9/0.7	63.0/0.75	3	2.20	0.077	0.996
2D	∞	1.25	∞	4.9/0.7	75.0/0.67	2.5~3	2.20	0.05	0.9996
2E	∞	1.25	12.0	4.9/0.7	63.0/0.75	4	2.20	0.025	0.997
2F	∞	1.25	5.0	4.9/0.7	63.0/0.75	3	2.20	0.014	0.9998
2G	∞	1.25	5.0	4.9/0.7	16.0/0.75	7	2.20	0.006	0.997
2H	∞	1.25	2.0	4.9/0.7	63.0/0.75	5~6	2.20	0.0056	0.995
2I	∞	1.25	2.0	4.9/0.7	16.0/0.75	8	2.20	0.0026	0.999
2J	∞	1.25	0.5	4.9/0.7	63.0/0.75	6	2.20	0.0015	0.999
3A	∞	1.25	∞	9.7/0.63	75.0/0.67	4~5	1.90	0.199	0.997
3B	∞	1.25	12.0	9.7/0.63	63.0/0.75	4.5	1.90	0.135	0.996
3C	∞	1.25	5.0	9.7/0.63	63.0/0.75	3~4	1.90	0.085	0.998
3D	∞	1.25	2.0	9.7/0.63	63.0/0.75	4	2.20	0.0177	0.994
3E	∞	1.25	0.5	9.7/0.63	63.0/0.75	4	2.20	0.0045	0.993
4A	∞	1.25	∞	5.0/0.28	75.0/0.67	5~5.5	2.20	0.068	0.998
4B	∞	1.25	12.0	5.0/0.28	63.0/0.75	7	2.20	0.032	0.997
4C	∞	1.25	5.0	5.0/0.28	63.0/0.75	8.5	2.20	0.016	0.994
4D	∞	1.25	2.0	5.0/0.28	63.0/0.75	8~9	2.20	0.007	0.996
4E	∞	1.25	0.5	5.0/0.28	63.0/0.75	7.5	2.20	0.0018	0.997
5A	∞	1.25	∞	5.1/0.18	75.0/0.67	5~7	2.20	0.077	0.99998
5B	∞	1.25	12.0	5.1/0.18	63.0/0.75	7	2.20	0.035	0.997
5C	∞	1.25	5.0	5.1/0.18	63.0/0.75	7~9	2.20	0.018	0.997
5D	∞	1.25	2.0	5.1/0.18	63.0/0.75	8.5~9	2.20	0.0075	0.996
5E	∞	1.25	0.5	5.1/0.18	63.0/0.75	8	2.20	0.002	0.999
6A	0.8	2.4	3.3	3.4/0.67	63.0/0.75	5~6	2.20	0.05	0.995
6B	3.3	2.4	8.0	3.4/0.67	63.0/0.75	1~4	2.20	0.025	0.993
6C	∞	2.4	∞	3.4/0.67	75.0/0.67	2.5~5	2.20	0.014	0.998
6D	∞	2.4	8.0	3.4/0.67	63.0/0.75	5.5	2.20	0.005	0.995
6E	∞	2.4	3.3	3.4/0.67	63.0/0.75	5.5~8.5	2.20	0.0025	0.998
6F	∞	2.4	0.8	3.4/0.67	63.0/0.75	6~10	2.20	0.00059	0.995
7A	3.3	2.4	8.0	7.3/0.73	63.0/0.75	2~5	2.10	0.094	0.9999
7B	8	2.4	19.0	7.3/0.73	63.0/0.75	3	2.10	0.074	0.999
7C	∞	2.4	∞	7.3/0.73	75.0/0.67	1.5~4	2.10	0.055	0.997
7D	∞	2.4	19.0	7.3/0.73	63.0/0.75	5.5	2.10	0.038	0.995
7E	∞	2.4	8.0	7.3/0.73	63.0/0.75	5~6	2.10	0.025	0.994
7F	∞	2.4	3.3	7.3/0.73	63.0/0.75	3~7	2.20	0.009	0.992
7G	∞	2.4	2.0	7.3/0.73	63.0/0.75	5~6	2.20	0.006	0.996
7H	∞	2.4	0.8	7.3/0.73	63.0/0.75	5	2.20	0.0025	0.998
8A	∞	2.4	∞	16.5/0.69	75.0/0.67	4~5	2.20	0.086	0.9999
8B	∞	2.4	19.0	16.5/0.69	63.0/0.75	3.5	1.90	0.105	0.994
8C	∞	2.4	8.0	16.5/0.69	63.0/0.75	3~3.5	1.95	0.07	0.992
8D	∞	2.4	3.3	16.5/0.69	63.0/0.75	2~4	2.00	0.035	0.999
8E	∞	2.4	0.8	16.5/0.69	63.0/0.75	2.5~5	2.00	0.0095	0.989

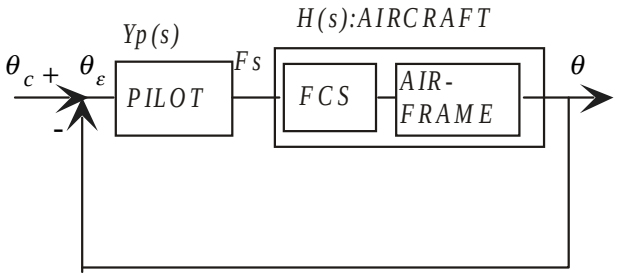

Fig.1 Pitch attitude tracking feedback system.

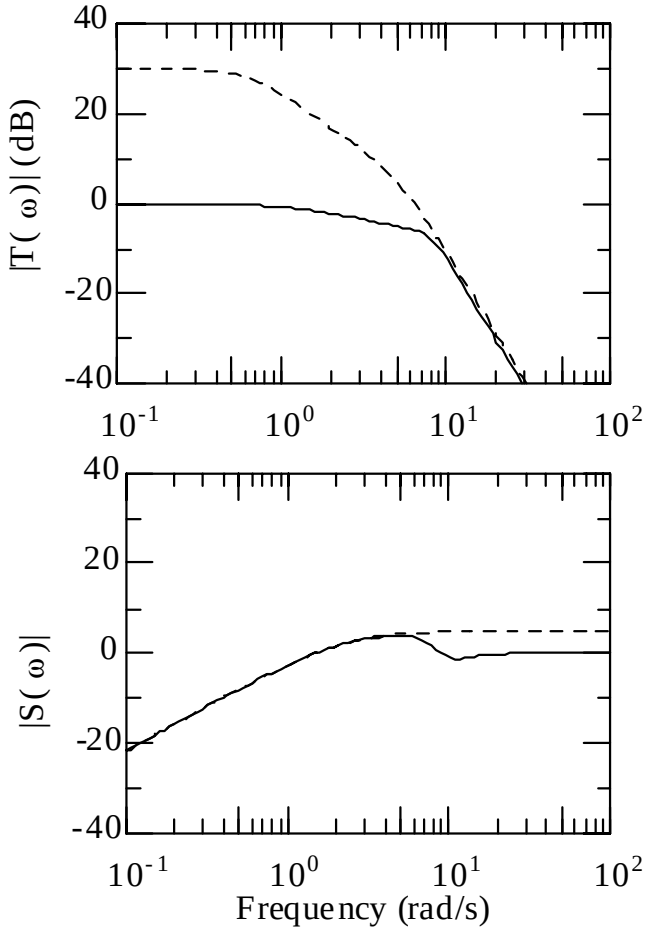

Fig.2a H_∞-optimal results for configuration 2D;
——— : *T*, *S* , ------ : W^{-1}, V^{-1}.

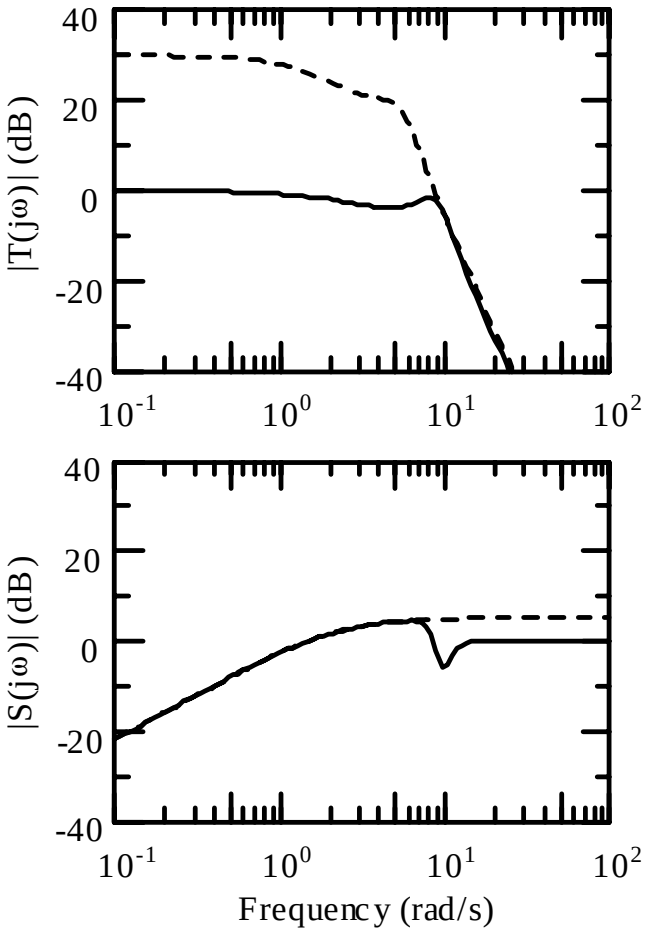

Fig.2b H_∞-optimal results for configuration 5C;
——— : *T*, *S* , ------ : W^{-1}, V^{-1}.

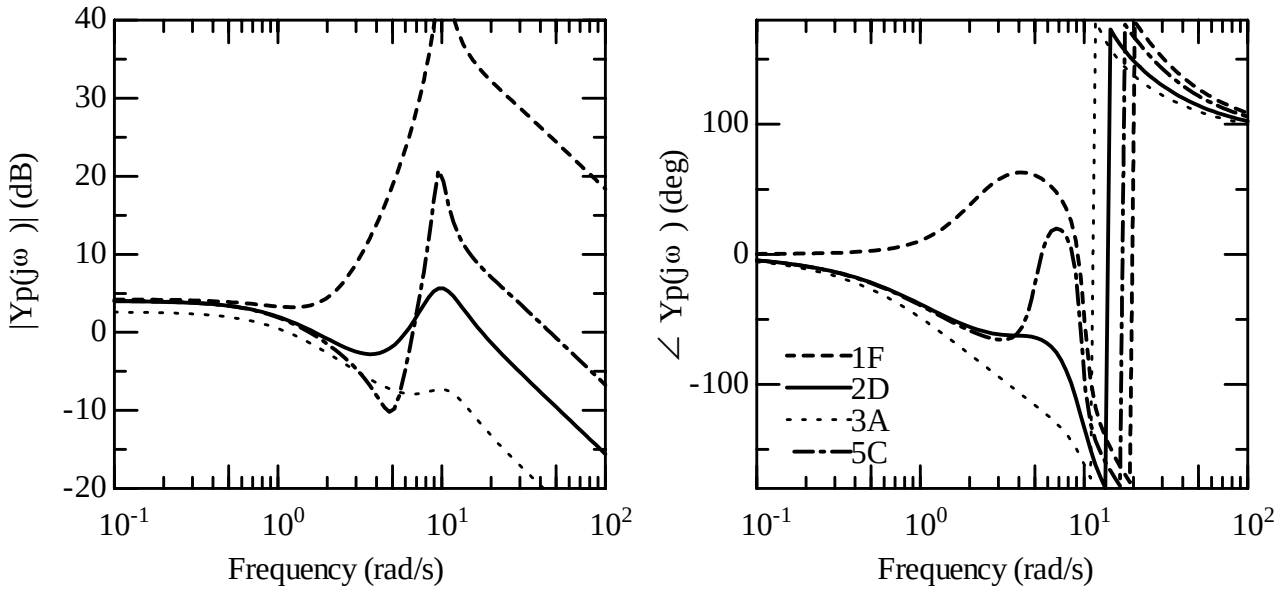

Fig.3 Bode diagrams of H_∞-optimal pilot models for configurations 1F, 2D, 3A, and 5C.

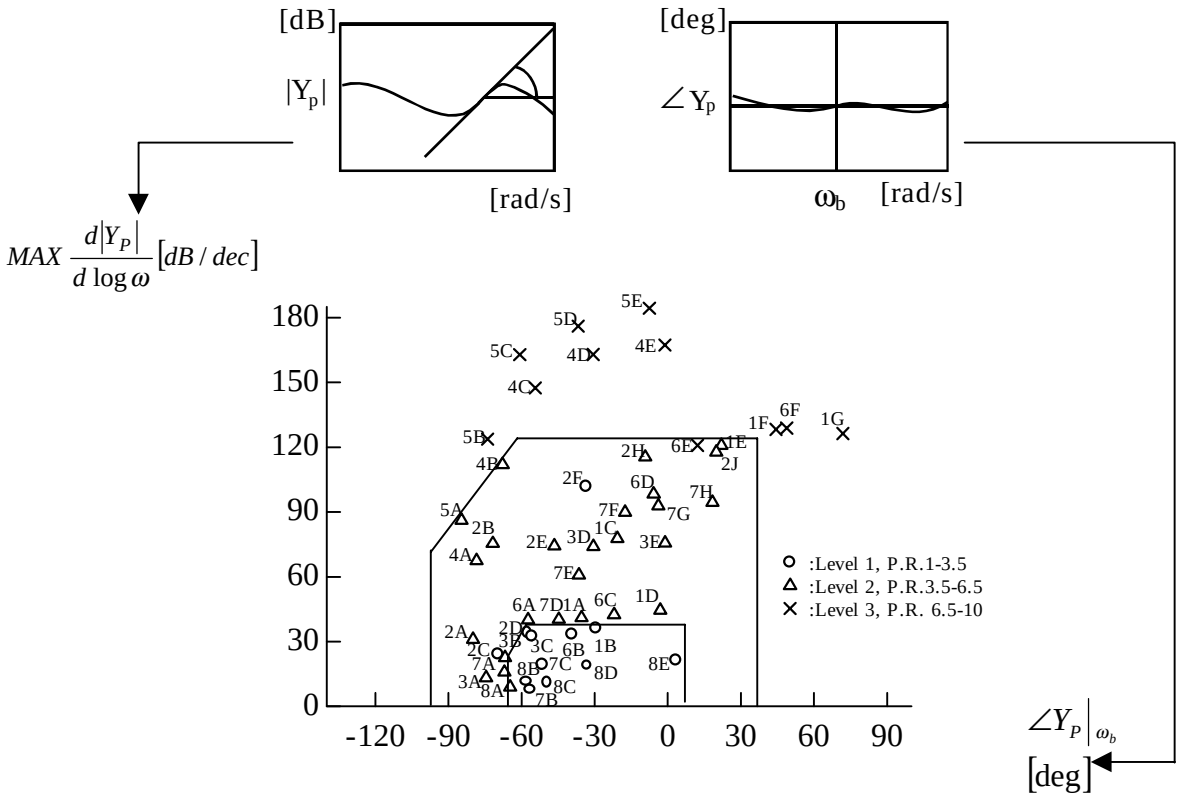

Fig.4 Neal-Smith data in the plane of the H_∞-pilot model's maximum gain gradient vs. phase compensation at ω_b.

Appendix

The mixed-sensitivity problem of Eq.(7) can be reduced to a model matching problem. According to Eq.(19), $\tilde{H}(s)$ first undergoes the coprime factorization as

$$\tilde{H}(s) = N(s)/M(s) \qquad \text{(A1)}$$

$M(s), N(s) \in RH_\infty$ (stable, proper, real-rational functions).

The controller $G(s)$ that achieves internal stability is given by the Youla parametrization

$$G(s) = (X + MQ)/(Y - NQ) \qquad \text{(A2)}$$

where $X, Y \in RH_\infty$ are the solutions to the Bezout equation

$$N(s)X(s) + M(s)Y(s) = 1, \qquad \text{(A3)}$$

and $Q(s)$ is an unknown parameter to be determined so as to be H_∞-optimal. Using Eq.(A2), the H_∞-norm of Eq.(7) reduces to

$$\left\| VM(Y - NQ)|^2 + |W_\mu N(X + MQ)|^2 \right\|_\infty \qquad \text{(A4)}$$

where

$$W_\mu \overline{W}_\mu = W\overline{W} + \mu\bar{\mu}s\bar{s}\frac{M\overline{M}}{N\overline{N}} \qquad \text{(A5)}$$

$$\overline{A(s)} = A(-s).$$

Taking into consideration the condition required for the model matching method that

$$W_\mu \overline{W}_\mu M \overline{M} N \overline{N} \in RH_\infty, \qquad \text{(A6)}$$

the simplest form of $\mu(s)$ can be Eq.(14). Further arrangement of Eq.(A4) reduces the performance index of Eq.(7) finally to

$$\text{minimize} \left\| T_1 - T_2 Q \right\|_\infty < 1 \qquad \text{(A7)}$$

$$T_1, T_2 \in RH_\infty.$$

This is a model matching problem, the solving procedure of which is well developed[8, 10].

To test the validity of this H_∞-approach, where a control rate related term is included in the performance index, H_∞-optimal pilot models are fitted to experimental pilot describing functions[11]. The controlled element dynamics used for this comparison are basic three kinds : $H(s)$=1, 1/s, and 1/s^2. The procedure of obtaining the H_∞-optimal pilot models is the same as is described in the text. However, the best fittings are attained by employing weighting functions that are different in relative order from those in the text, basically due to the consideration that the H_∞-optimal model features the roll-off characteristic of –20dB/dec in a high-frequency range. The results are shown in Figs.A1, A2, and A3. Weighting functions and parameter values for each controlled element are as follows :

1. $H(s)$=1

$\omega_b = 9.0$ rad/s, $\tau = 0.15$ s, $\angle T|_{\omega_b} = -90.8$ deg

$$V(s) = \left(2.4 \cdot 10^{-10/20} \cdot \sqrt{\frac{1+\omega_b{}^2}{2}} \right) \frac{\frac{1}{\omega_b}s + 1}{s + 1}$$

$$W(s) = 10^{-10/20} \frac{\frac{1}{\omega_b}s + 1}{\frac{10^{-60/20}}{\omega_b}s + 1}$$

$$\mu(s) = (10^{-8}) \frac{1}{1 + (10^{-5})s}$$

2. $H(s)$=1/s

$\omega_b = 7.0$ rad/s, $\tau = 0.15$ s, $\angle T|_{\omega_b} = -89.9$ deg

$$V(s) = \left(10^{-4.9/20} \cdot \sqrt{\frac{(1+\frac{1}{4}\omega_b{}^2)(1+10^8\omega_b{}^2)}{2}} \right) \frac{(\frac{1}{\omega_b}s+1)^2}{(\frac{1}{2}s+1)(10^4 s+1)}$$

$$W(s) = 10^{-17/20} \left\{ \left(\frac{s}{\omega_b} \right)^2 + \frac{2 \times 0.71}{\omega_b}s + 1 \right\}$$

$$\mu(s) = 0.0014 \frac{1}{1 + (10^{-5})s}$$

3. $H(s)$=1/s^2

$\omega_b = 3.0$ rad/s, $\tau = 0.21$ s, $\angle T|_{\omega_b} = -89.8$ deg

$$V(s) = \left(1.2 \cdot 10^{-10/20} \cdot \frac{1+10^8\omega_b{}^2}{2} \right) \frac{(\frac{1}{\omega_b}s+1)^2}{(10^4 s+1)^2}$$

$$W(s) = 10^{-10/20} \frac{\frac{1}{\omega_b}s + 1}{\frac{10^{-60/20}}{\omega_b}s + 1}$$

$$\mu(s) = 0.002 \frac{1}{1 + (4 \cdot 10^{-5})s}$$

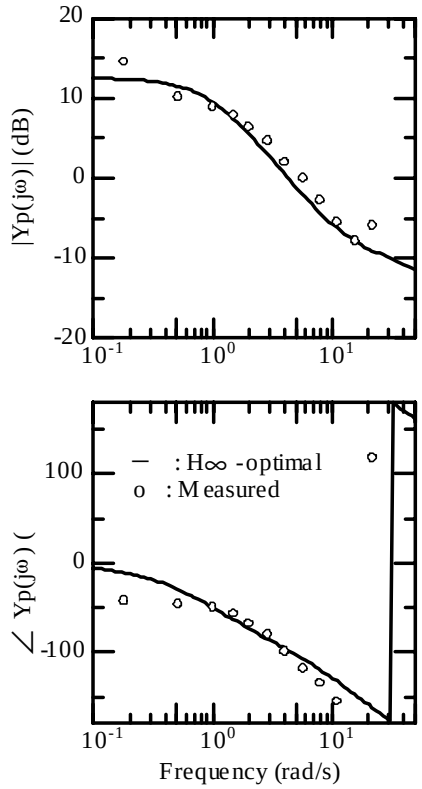

Fig.A1 H_∞-optimal vs. measured pilot describing functions : $H(s)=1$.

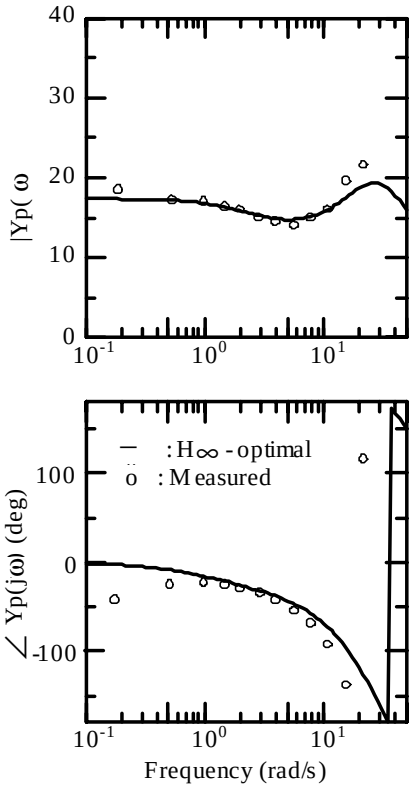

Fig.A2 H_∞-optimal vs. measured pilot describing functions : $H(s)=1/s$.

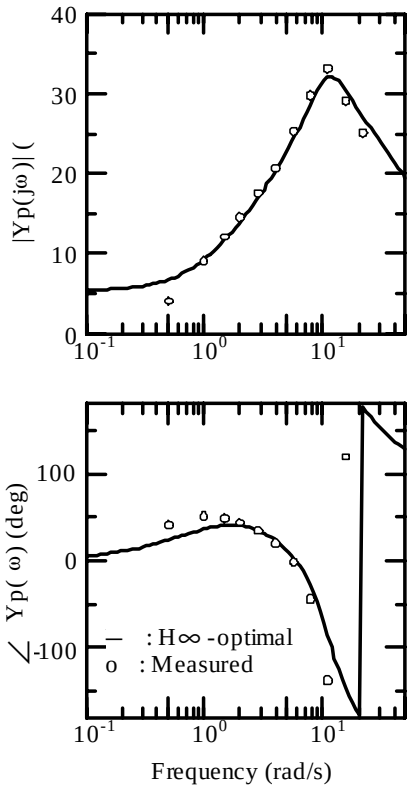

Fig.A3 H_∞-optimal vs. measured Pilot describing functions : $H(s)=1/s^2$.